Western blotting

COS7 cells were transfected with pcDNA3.1 Zac1 using Lipofectamine (Invitrogen, Carlsbad, CA). Cell extracts were isolated 24 h after transfection and separated into nuclear and cytosolic fractions. Fractionated protein lysates were resolved by SDS-PAGE and transferred to a PVDF membrane, followed by immunoblotting with rabbit anti-Zac1 antibody (Santa Cruz Biotechnology) at a dilution of 1:1,000 and horseradish peroxidase-conjugated anti-goat IgG, followed by development with the SuperSignal West Pico Chemiluminescent reagent (Pierce, Rockford, IL).

IP-western blot analysis

Total cell lysate was prepared from neonatal mouse hearts. IP-western blot analysis was performed essentially as described previously using anti-Zac1 and anti-Nkx2-5 for hearts lysate.

Plasmids

The Zac1-expressing plasmids were generated through conventional or PCR-based cloning. Deletion mutants were constructed by PCR-based mutagenesis and subcloning of the DNA fragments into the pcDNA3.1 expression vector. Site-directed mutagenesis was performed using the QuickChange kit (Stratagene, La Jolla, CA). The reporter plasmids (ANP-luciferase, BNP-luciferase, and α-MHC-luciferase) were kindly provided from Dr. E.N. Olson. The *Zac1* promoter was cloned using PCR-based techniques from a BAC clone into the pGL3 basic vector (Promega, Madison, WI). For mammalian hybrid assay, pBIND vector and pG5luc vector were purchased from Promega.

Cell culture, transfection, and luciferase assay

COS-7 cells plated in DMEM with 10% FBS were transfected with Lipofectamine (Invitrogen) according to the manufacturer's instructions. Unless otherwise indicated, 100ng of reporter and 100ng of each activator plasmid were used. The DNA doses represented by the ramp symbol indicate 0, 30, 100 and 300ng of plasmid. The total amount of DNA per well was kept constant by adding the corresponding amount of expression vector without a cDNA insert. CMV-*Renilla* luciferase was used as an internal control, to normalize for variations in transfection efficiency. All the proteins were expressed at very similar levels, as confirmed by Western blotting.

EMSA

Nuclear extracts were collected from COS7 cells that overexpressed Zac1. Double-stranded oligonucleotides for the Zac1-binding sequence '(5 -GCATCTTCTGCTGGCCGCCG-3') were synthesized, and the two complementary oligonucleotides were annealed and labeled with [α-^{32}P]-dATP using the Klenow enzyme. Labeled probes were incubated with 5 ml of nuclear extracts and 2mg of poly(dI-dC) in 20 ml of binding buffer [10 mM Tris-HCl (pH 7.5), 50 mM NaCl, 10% glycerol, 0.5 mM dithiothreitol, 0.05% Nonidet P-40] for 30 min at room temperature. The protein/DNA mixture was resolved on a 5% polyacrylamide gel in 0.5 Tris borate/EDTA buffer at 4°C for 2 h at 150 V.

ChIP assay

For the *in vivo* ChIP experiments, extracts were prepared from five neonatal rat wild-type hearts for independent experiments. For the ChIP assays, we used the Chromatin Immunoprecipitation Assay Kit (Upstate Biotechnology, Lake Placid, NY) and followed the instructions of the supplier. Primer in PCR reactions is 5'-ACAAGCTTCGCTGGACTGAT-3' and 5'-TCTCGGCTCACTCTCTGGTT-3' (-148 +43), 5'-CCTGACTGCTAACAGGGACA-3' and 5'-

TGTCAGGGGCTCCAAATAAG-3′ (-576 -398), 5′-GAGAGGAGCTGGACCATGAG-3′ and 5′-TTGAAAGCGTGAGGACTTGA-3′ (-2907 -2728). The amplified region corresponded to the rat ANP promoter, which encompasses the Zac1-binding sites.

Glutathione S-transferase (GST) pulldown assay

Murine Zac1 cDNA and several DNA fragments encoding Zac1 were subcloned into the pGex-6P vector (Amersham Biosciences). GST fusion proteins were isolated by standard procedures. The plasmids that contained the deletion mutants of Nkx2-5 were gifted by Dr. I. Komuro. Proteins translated *in vitro* were labeled with [^{35}S]-methionine in the coupled transcription-translation T7 reticulocyte lysate system (Promega), and assayed for binding to the GST-fusion proteins.

RT-PCR and real-time quantitative PCR

Total RNA was extracted using the Trizol reagent (Invitrogen), and RT-PCR was performed as described previously. At least five replicates were processed for each assay. *GAPDH* was used as an internal control. For quantitative analysis of *Nkx2-5*, *GATA4*, *ANP*, *MLC2v*, and *MLC2a* expression, the respective cDNA was used as the template in a TaqMan real-time PCR assay using the ABI Prism 7700 sequence detection system (Applied Biosystems) according to the manufacturer's instructions. All samples were run in triplicate. The data were normalized to *GAPDH* expression. The primers and TaqMan probe for *Nkx2-5*, *GATA4*, *ANP*, *MLC2v*, *MLC2a* and *Zac1* were Mm00657783_m1, Mm00484689_m1, Mm01255747_g1, Mm00440384_m1, Mm00491655_m1, and Mm00494251_m1, respectively.

Generation of mutant mice

The *Zac1*-mutated mice were generated by Lexicon Pharmaceuticals from ES cells that corresponded to OST181461 (OmniBank sequence tag) and that were targeted by gene trapping. The gene-trapping vector contained a retroviral 5 -end long terminal repeat (LTR), a splice acceptor sequence, neomycin gene (Neo), and partial first intron of the murine *Bruton's tyrosine kinase* (*Btk*) gene as the 3 -trapping component, rather than a selectable marker, which was regulated by the 3-phosphoglycerate kinase 1 (PGK-1) gene promoter, a splice donor sequence, and a 3'-LTR[2]. Retroviral infection, selection, and screening of the ES cells were performed as previously described. The gene-trapping vector was inserted at the third intron of the *Zac1* gene (corresponding to OST181461) in the ES cells, as detected by inverse-PCR. ES cells were selected for blastocyst injection into C57BL/6 mice to produce chimeric mice. Heterozygous and homozygous animals were analyzed along with littermate control animals.

Statistical Analyses

Values are presented as mean ± SEM. Statistical significance was evaluated with the unpaired Student *t* test for comparisons between 2 mean values. A chi squared analysis for comparisons between 2 groups. Comparisons between >3 groups were performed with ANOVA. A value of $P<0.05$ was considered significant. *p<0.05, **P<0.01, NS; not significant.

References

1. Yuasa S, Itabashi Y, Koshimizu U, Tanaka T, Sugimura K, Kinoshita M, Hattori F, Fukami S, Shimazaki T, Ogawa S, Okano H, Fukuda K. Transient inhibition of BMP signaling by Noggin induces cardiomyocyte differentiation of mouse embryonic stem cells. *Nat Biotechnol.* 2005;23:607-611.

2. Zambrowicz BP, Friedrich GA, Buxton EC, Lilleberg SL, Person C, Sands AT. Disruption and sequence identification of 2,000 genes in mouse embryonic stem cells. *Nature.* 1998;392:608-611.

Supplement Material

Online Figure I

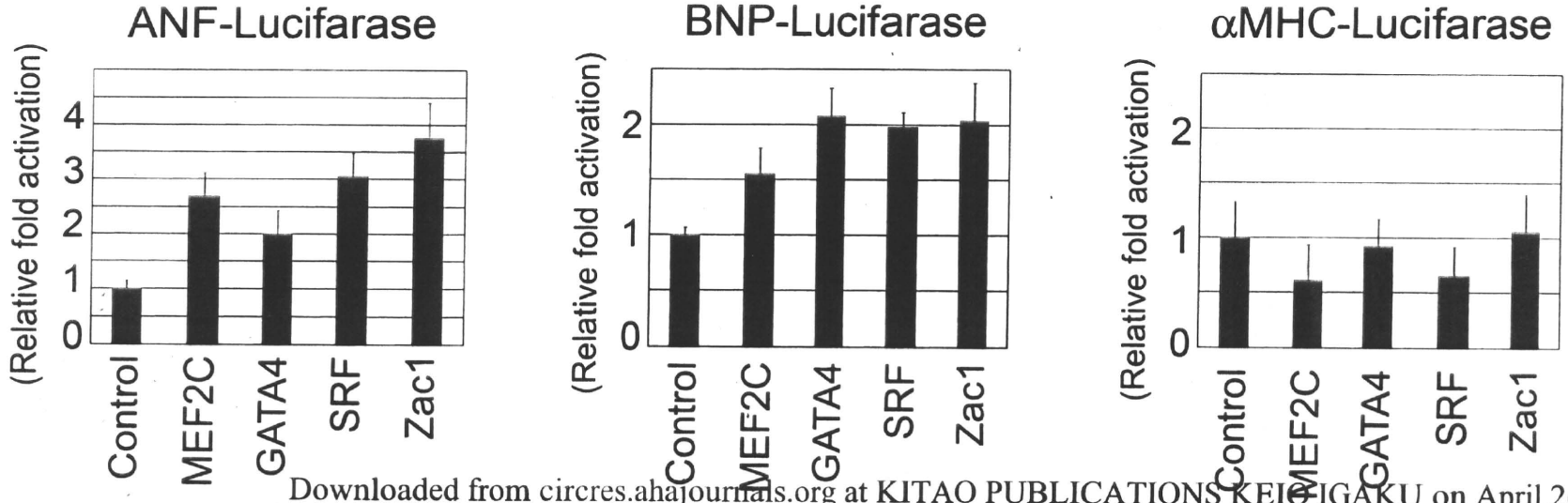

Brief Ultrarapid Communication

The (Pro)renin Receptor/ATP6AP2 is Essential for Vacuolar H^+-ATPase Assembly in Murine Cardiomyocytes

Kenichiro Kinouchi, Atsuhiro Ichihara, Motoaki Sano, Ge-Hong Sun-Wada, Yoh Wada, Asako Kurauchi-Mito, Kanako Bokuda, Tatsuya Narita, Yoichi Oshima, Mariyo Sakoda, Yoshitaka Tamai, Hiromu Sato, Keiichi Fukuda, Hiroshi Itoh

Rationale: The (pro)renin receptor [(P)RR], encoded in *ATP6AP2*, plays a key role in the activation of local renin-angiotensin system (RAS). A truncated form of (P)RR, termed M8.9, was also found to be associated with the vacuolar H^+-ATPase (V-ATPase), implicating a non–RAS-related function of ATP6AP2.

Objective: We investigated the role of (P)RR/ATP6AP2 in murine cardiomyocytes.

Methods and Results: Cardiomyocyte-specific ablation of *Atp6ap2* resulted in lethal heart failure; the cardiomyocytes contained RAB7- and lysosomal-associated membrane protein 2 (LAMP2)-positive multivesicular vacuoles, especially in the perinuclear regions. The myofibrils and mitochondria remained at the cell periphery. Cardiomyocyte death was accompanied by numerous autophagic vacuoles that contained undigested cellular constituents, as a result of impaired autophagic degradation. Notably, ablation of *Atp6ap2* selectively suppressed expression of the V_O subunits of V-ATPase, resulting in deacidification of the intracellular vesicles. Furthermore, the inhibition of intracellular acidification by treatment with bafilomycin A1 or chloroquine reproduced the phenotype observed for the (P)RR/ATP6AP2-deficient cardiomyocytes.

Conclusions: Genetic ablation of *Atp6ap2* created a loss-of-function model for V-ATPase. The gene product of *ATP6AP2* is considered to act as in 2 ways: (1) as (P)RR, exerting a RAS-related function; and (2) as the V-ATPase-associated protein, exerting a non–RAS-related function that is essential for cell survival. (*Circ Res*. 2010;107:30-34.)

Key Words: V-ATPase ■ autophagy ■ heart failure ■ bafilomycin ■ renin-angiotensin system

Activation of the (pro)renin receptor [(P)RR], the gene product of ATP6AP2, plays a key role in the local renin-angiotensin system (RAS). We have shown that (P)RR activation is involved in the development of cardiac fibrosis and proteinuria in hypertension and diabetes. Interestingly, a truncated form of (P)RR, termed M8.9, was also found to be associated with the vacuolar H+-ATPase (V-ATPase), implicating a non–RAS-related function of the gene products of ATP6AP2.[1] In the present study, we show that gene products of ATP6AP2 are essential for cardiomyocyte survival via regulating V-ATPase function.

Methods

We generated conditional knockout (CKO) mice in which exon 2 of the *Atp6ap2* gene was flanked by loxP sites (Online Figure I). *Atp6ap2*-floxed mice were bred with mice that expressed the Cre recombinase under the control of the cardiomyocyte-specific α-myosin heavy chain (α-MHC) promoter (Online Figure II).[2,3] The resulting $Atp6ap2^{lox/Y}$, $\alpha MHC\text{-}Cre^{+/0}$ mice represent cardiac-specific *Atp6ap2* CKO mice. The control male mice were littermates that were heterozygous for α-MHC-Cre ($\alpha MHC\text{-}Cre^{+/0}$; $Atp6ap2^{+/Y}$), thereby excluding Cre-mediated toxicity as the basis for phenotypic disparity. An expanded Methods section is available in the Online Data Supplement at http://circres.ahajournals.org.

Results and Discussion

The CKO mice were born at the expected mendelian frequency, without any gross cardiac anomalies being noted in the newborn mice, although cardiomyocyte-specific ablation of *Atp6ap2* inevitably resulted in heart failure and the mice died within 3 weeks of birth (Figure 1a through 1c). Ventric-

Original received May 19, 2010; revision received June 1, 2010; accepted June 3, 2010. In May 2010, the average time from submission to first decision for all original research papers submitted to *Circulation Research* was 14.6 days.

From the Department of Endocrinology, Metabolism, and Nephrology (K.K., A.I., A.K.-M., K.B., T.N., M.S., H.I.), the Department of Endocrinology and Anti-Aging Medicine and Internal Medicine (A.I., Y.O.), and the Department of Cardiology (M.S., K.F.), Keio University School of Medicine, Tokyo, Japan; Precursory Research for Embryonic Science and Technology (PRESTO) (M.S.), Japan Science and Technology Agency, Saitama, Japan; the Department of Biochemistry (G.-H.S.-W.), Faculty of Pharmaceutical Sciences, Doshisha Women's College, Kyoto, Japan; the Division of Biological Sciences (Y.W.), Institute of Scientific and Industrial Research, Osaka University, Osaka, Japan; BANYU Tsukuba Research Institute (Y.T., H.S.), Ibaraki, Japan; and Charles River Laboratories JAPAN (Y.T.), Kanagawa, Japan.

Brief UltraRapid Communications are designed to be a format for manuscripts that are of outstanding interest to the readership, report definitive observations, but have a relatively narrow scope. Less comprehensive than Regular Articles but still scientifically rigorous, BURCs present seminal findings that have the potential to open up new avenues of research. A decision on BURCs is rendered within 7 days of submission.

Correspondence to Dr Atsuhiro Ichihara, Department of Endocrinology and Anti-Aging Medicine and Internal Medicine, Keio University School of Medicine, 35 Shinanomachi Shinjuku-ku, Tokyo, 160-8582, Japan. E-mail atzichi@sc.itc.keio.ac.jp

Circulation Research is available at http://circres.ahajournals.org DOI: 10.1161/CIRCRESAHA.110.224667

ular functions were severely impaired on postnatal day (PD)18 (fractional shortening, 12.87±4.73% versus 27.69±0.58% for CKO versus control; n=3; $P<0.05$) (Figure 1d, Online Video I). The CKO mice showed significantly increased ratios of heart weight—to–body weight beginning on PD14 (Figure 1e). The levels of cardiac stress markers, including atrial natriuretic peptide, brain natriuretic peptide, α-skeletal actin, connective tissue growth factor, and monocyte chemoattractant protein-1, were increased as early as PD10 (Figure 1f). Histological examination of the CKO mice on PD18 revealed that clusters of degenerating cardiomyocytes with extensive vacuolation, especially in the perinuclear region, were embedded in areas of replacement fibrosis (Figure 2a and 2b). Electron microscopic examination of the CKO cardiomyocytes revealed perinuclear accumulations of numerous multivesicular vacuoles (Figure 2c and 2d). The myofibrils and mitochondria were located exclusively at the cell periphery. In addition, we observed large, electron-dense autophagic vacuoles that contained partially digested or undigested cellular constituents, such as mitochondria and aberrant vacuoles, scattered in the field of cell debris around the perinuclear region (Online Figure III). The accumulation of microtubule-associated protein 1 light chain 3 (LC3)-II (a phosphatidylethanolamine conjugate) and p62/SQSTM1, as well as the induction of genes in response to amino acid starvation (eg, the genes for asparagine synthetase, activating transcription factor 4, and C/EBP homologous protein) reflected defective autophagic protein degradation in the CKO mice (Figure 2e and 2f).

To examine the underlying cellular mechanism responsible for cardiac death, we examined the role of the ATP6AP2 protein in the function of V-ATPase, which maintains a

Non-standard Abbreviations and Acronyms

α-MHC	α-myosin heavy chain
CKO	conditional knockout
LAMP2	lysosomal-associated membrane protein 2
LC3	microtubule-associated protein 1 light chain 3
MEFs	mouse embryonic fibroblasts
PD	postnatal day
(P)RR	(pro)renin receptor
RAS	renin-angiotensin system
V-ATPase	vacuolar H^+-ATPase

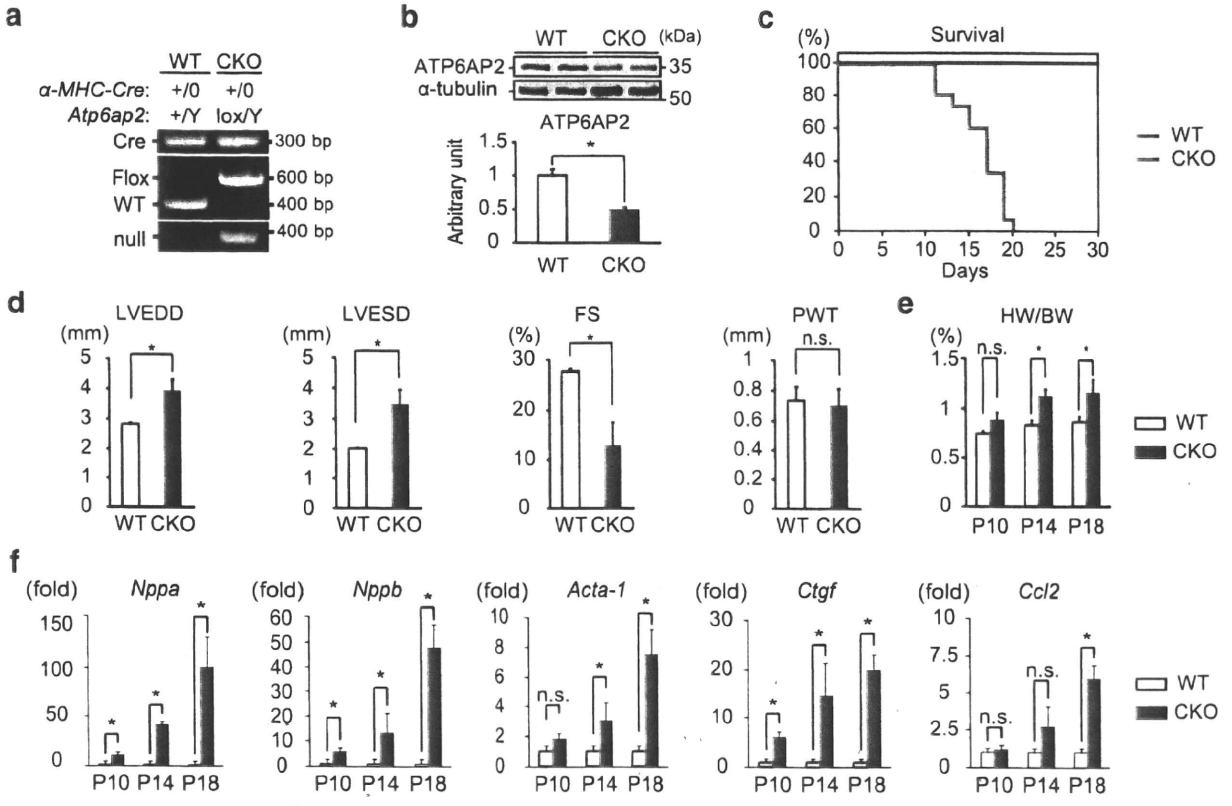

Figure 1. Cardiomyocyte-specific ablation of *Atp6ap2* inevitably caused heart failure. a, PCR genotyping of myocardial DNA, showing conditional deletion of floxed *Atp6ap2* contingent on coinheritance of *α-MHC-Cre*. **b**, ATP6AP2 protein was deleted from myocardium. *$P<0.05$ vs WT control. **c**, Kaplan-Meier survival curve showing lethality by 3 weeks of birth in the CKO mice. **d**, Echocardiographic data representing left ventricular dilation and compromised contraction in the CKO hearts on PD18. Values represent means±SEM. LVEDD indicates left ventricular end-diastolic diameter; LVESD, left ventricular end-systolic diameter; FS, fractional shortening; and PWT, posterior wall thickness. n=3, *$P<0.05$ vs WT control. **e**, HW/BW ratios of WT and CKO. n=4, *$P<0.05$ vs WT control. **f**, Expression of cardiac stress genes in the CKO mice. *Nppa* indicates atrial natriuretic peptide; *Nppb*, brain natriuretic peptide; *Acta-1*, α-skeletal actin; *Ctgf*, connective tissue growth factor; and *Ccl2*; monocyte chemotactic protein-1. n=4, *$P<0.05$ vs WT control.

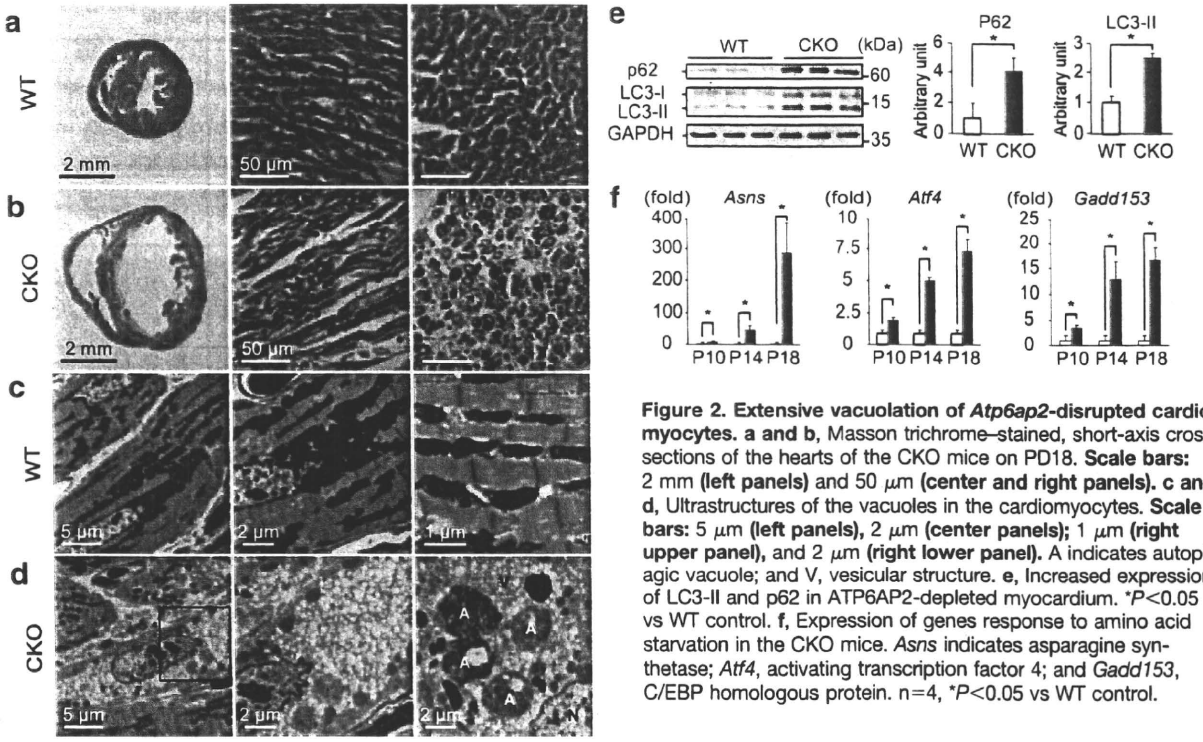

Figure 2. Extensive vacuolation of *Atp6ap2*-disrupted cardiomyocytes. a and b, Masson trichrome–stained, short-axis cross sections of the hearts of the CKO mice on PD18. **Scale bars:** 2 mm **(left panels)** and 50 μm **(center and right panels). c and d,** Ultrastructures of the vacuoles in the cardiomyocytes. **Scale bars:** 5 μm **(left panels),** 2 μm **(center panels);** 1 μm **(right upper panel),** and 2 μm **(right lower panel).** A indicates autophagic vacuole; and V, vesicular structure. **e,** Increased expression of LC3-II and p62 in ATP6AP2-depleted myocardium. *$P<0.05$ vs WT control. **f,** Expression of genes response to amino acid starvation in the CKO mice. *Asns* indicates asparagine synthetase; *Atf4*, activating transcription factor 4; and *Gadd153*, C/EBP homologous protein. n=4, *$P<0.05$ vs WT control.

luminal acidic environment in the intracellular vesicular compartments (Figure 3a).[4,5] Mouse embryonic fibroblasts (MEFs) were obtained from male mice that were hemizygous for the floxed *Atp6ap2* allele. The *Atp6ap2* gene was ablated by infecting the MEFs with the Cre adenovirus (Ad-Cre) (Online Figure IVa). Quantitative PCR and Western blot analyses showed that ≥90% of the ATP6AP2 protein was missing in the floxed MEFs after Ad-Cre treatment, as compared with the wild-type (WT) MEFs (Online Figure IVb and Figure 3b). V-ATPase is a large multisubunit complex that is organized into the V_1 and V_O sectors. In mammals, the V_1 sector is composed of 8 different subunits (A through H), whereas the V_O sector contains 6 different subunits (a, c, c″, d, e, and the accessory subunit Ac45[6]) (Figure 3a). Western blot and immunohistochemical analyses revealed that the levels of subunits a1, a2, a3, and c were significantly decreased in the floxed MEFs after Ad-Cre infection, as compared with the WT MEFs (Figure 3b and 3c). In contrast, the level of V_1 subunit E2 was unaffected. Consistent with these findings, LysoTracker staining revealed that the loss of ATP6AP2 was accompanied by impaired vesicular acidification (Figure 3c). Taken together, these findings suggest that genetic ablation of ATP6AP2 selectively affects the stability and assembly of the V_O subunits, thereby compromising vesicular acidification.

Consistent with the findings observed for cultured cells, ATP6AP2-depleted hearts revealed that the characteristic perinuclear vacuoles in the cardiomyocytes were positive for late endosomal/lysosomal markers RAB7 and/or LAMP2 (Figure 3d). The levels of the c-subunit of the V_O sector but not the E2 subunit of the V1 sector markedly reduced in the CKO cardiomyocytes.

To investigate whether disruption of intracellular acidification accounts for the phenotype of the ATP6AP2-deficient cardiomyocytes, we treated cultured cardiomyocytes with bafilomycin A1 or chloroquine. Sequential time-lapse microscopic analysis revealed that intracellular vacuoles accumulated over time (Figure 4; Online Video II). These vacuoles were positive for RAB7 (Figure 4). Interestingly, *Atp6ap2* mRNA expression in the cultured cardiomyocytes was strikingly upregulated after treatment with either bafilomycin A1 or chloroquine (Online Figure V).

The biogenesis of the multisubunit complex of V-ATPase requires the coordinated association of V_1 subunits, which are synthesized in the cytosol, with V_O subunits, which are targeted to the vacuolar membrane. Studies in yeast cells have shown that the loss of a V_1 subunit has little effect on the stability of the remaining V_1 subunit, whereas the loss of any single V_O subunit affects the stability and assembly of the remaining V_O subunits. In yeast, several additional genes (*Vma12p*, *Vma21p*, and *Vma22p*) that are required for V-ATPase assembly have been identified.[7] The V_O subunits were detected at greatly reduced levels in the mutant cells that lacked these assembly factors, an effect that is similar to that observed after the loss of a V_O subunit.[8] Interestingly, there is no known yeast homolog of the mammalian ATP6AP2. It is possible that ATP6AP2 is an assembly chaperone of V-ATPase, representing a function that is unique to mammals. An alternative scenario is that ATP6AP2 is a component of the V_O sector itself rather than an assembling factor. *Atp6ap2* mRNA expression was upregulated in cells that were treated with bafilomycin A1 or chloroquine, which suggests that ATP6AP2 senses the acidity levels of the intracellular compartments and accordingly regulates V-ATPase activity.

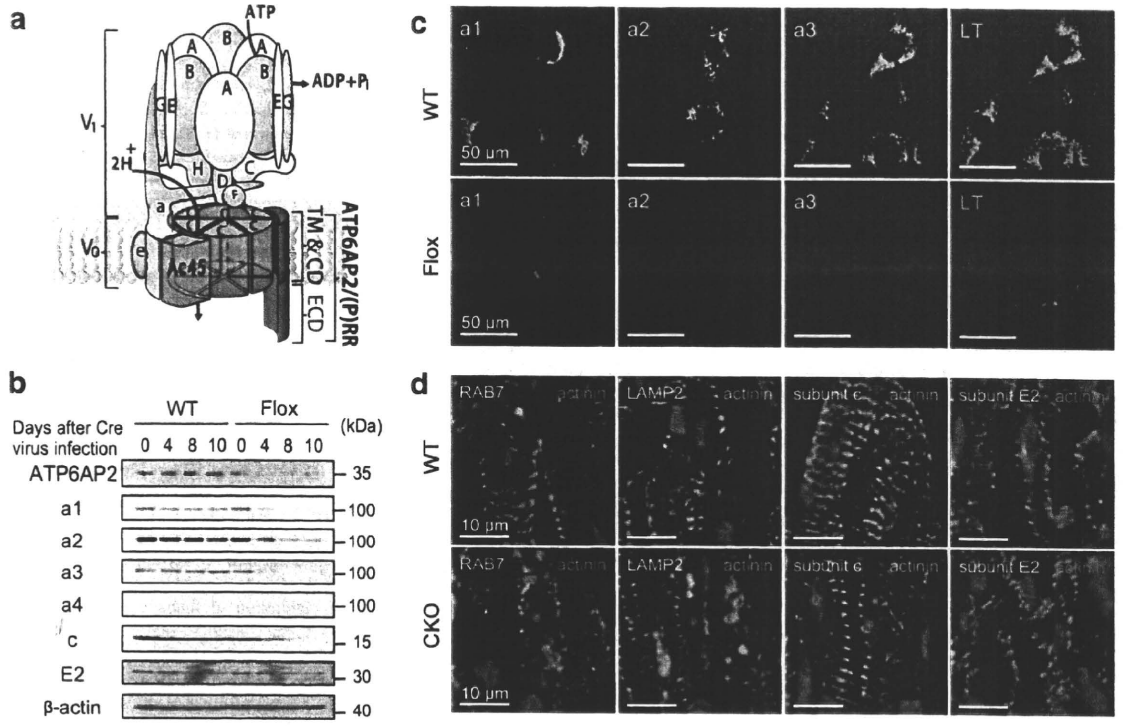

Figure 3. ATP6AP2 is indispensable for the assembly of V-ATPase. a, Structure of the V-ATPase and putative colocalization of ATP6AP2 and the V-ATPase. TM & CD indicates transmembrane and cytosolic domain; and ECD, extracellular domain. **b and c,** The levels of V_O subunits are decreased significantly in the floxed MEFs after deletion of the *Atp6ap2* gene. The V_1 subunit E2 appears to be unaffected. **c,** Defective acidification in the floxed MEFs after deletion of the *Atp6ap2* gene. **Scale bars:** 50 μm. **d,** Immunofluorescence staining of left ventricular tissues from WT and CKO mice on PD18. The vacuoles in the actinin-positive cardiomyocytes are RAB7-positive and LAMP2-positive. The levels of the c-subunit of the V_O sector of the V-ATPase are markedly reduced in the CKO cardiomyocytes, whereas the depletion of ATP6AP2 had no effect on the expression of the subunit E2 in cardiomyocytes. Nuclei were counterstained with DAPI **(blue). Scale bar:** 10 μm.

In conclusion, the gene product of *Atp6ap2* is considered to act in 2 ways: (1) as (P)RR, exerting an RAS-related function[9]; and (2) as the V-ATPase–associated protein, exerting a non–RAS-related function that is essential for cell survival.[10] The phenotypes observed after genetic ablation of *Atp6ap2* are ascribed to V-ATPase loss of function. Further characterizing the function of ATP6AP2 as an assembly chaperone of V-ATPase and the pathological function of

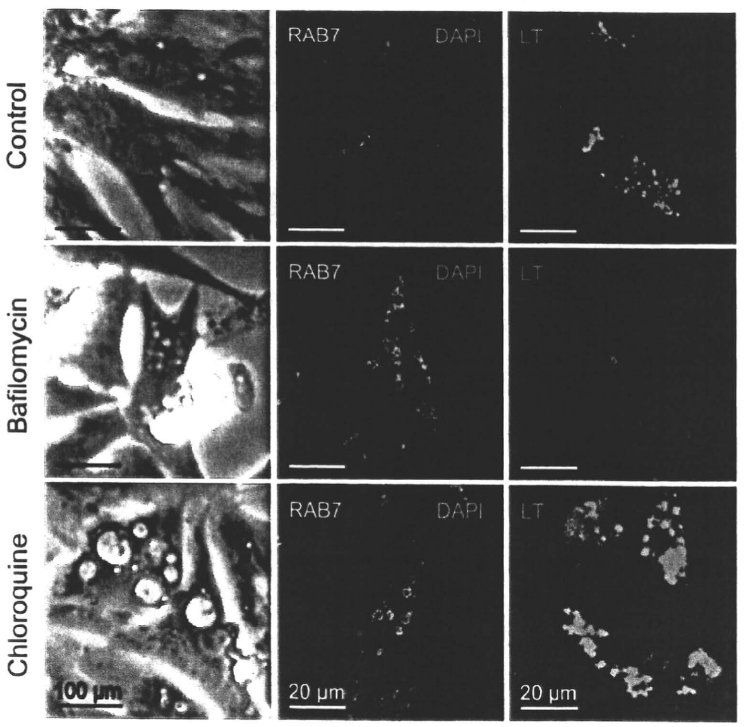

Figure 4. Inhibition of vesicular acidification by bafilomycin A1 or chloroquine mimics the in vivo cardiac phenotype that results from ablation of *Atp6ap2*. The rat cardiomyocytes were treated with bafilomycin A1 (100 nmol/L) or chloroquine (10 μmol/L) for 24 hours and then stained either with RAB7 plus DAPI or LysoTracker Red. Note that treatment with bafilomycin A1 or chloroquine reproduces the RAB7-positive intracellular vesicles by inhibiting vesicular acidification. **Scale bars:** 100 μm **(left panels)** and 20 μm **(center and right panels).**

(P)RR would require rescue experiments with the WT protein and with mutant proteins that lack the domain responsible for binding renin and prorenin.

Acknowledgments

We thank Shintaro Morizane, Tomohiro Matsuhashi, Shugo Tohyama, Hisayuki Hashimoto, Yoshiko Miyake, and Toshihiro Nagai for excellent technical assistance. We are also grateful to Noboru Mizushima and Genzou Takemura for their comments on the manuscript. Motoaki Sano and Hiroshi Itoh are core members of the Global Center of Excellence (GCOE) for Human Metabolomics Systems Biology, Ministry of Education, Culture, Sports, Science and Technology.

Sources of Funding

This work was supported by a grant from the Ministry of Education, Culture, Sports, Science and Technology (17390249 to A. I.) and a PRESTO (Metabolism and Cellular Function) grant from the Japanese Science and Technology Agency (to M. S.).

Disclosures

None.

References

1. Cruciat CM, Ohkawara B, Acebron SP, Karaulanov E, Reinhard C, Ingelfinger D, Boutros M, Niehrs C. Requirement of prorenin receptor and vacuolar H+-ATPase-mediated acidification for Wnt signaling. *Science*. 2010;327:459–463.
2. Gaussin V, Van de Putte T, Mishina Y, Hanks MC, Zwijsen A, Huylebroeck D, Behringer RR, Schneider MD. Endocardial cushion and myocardial defects after cardiac myocyte-specific conditional deletion of the bone morphogenetic protein receptor ALK3. *Proc Natl Acad Sci U S A*. 2002;99:2878–2883.
3. Sano M, Izumi Y, Helenius K, Asakura M, Rossi DJ, Xie M, Taffet G, Hu L, Pautler RG, Wilson CR, Boudina S, Abel ED, Taegtmeyer H, Scaglia F, Graham BH, Kralli A, Shimizu N, Tanaka H, Makela TP, Schneider MD. Menage-a-trois 1 is critical for the transcriptional function of PPARgamma coactivator 1. *Cell Metab*. 2007;5:129–142.
4. Forgac M. Structure and properties of the coated vesicle (H+)-ATPase. *J Bioenerg Biomembr*. 1992;24:341–350.
5. Sun-Wada GH, Wada Y, Futai M. Vacuolar H+ pumping ATPases in luminal acidic organelles and extracellular compartments: common rotational mechanism and diverse physiological roles. *J Bioenerg Biomembr*. 2003;35:347–358.
6. Supek F, Supekova L, Mandiyan S, Pan YC, Nelson H, Nelson N. A novel accessory subunit for vacuolar H(+)-ATPase from chromaffin granules. *J Biol Chem*. 1994;269:24102–24106.
7. Graham LA, Powell B, Stevens TH. Composition and assembly of the yeast vacuolar H(+)-ATPase complex. *J Exp Biol*. 2000;203:61–70.
8. Hirata R, Umemoto N, Ho MN, Ohya Y, Stevens TH, Anraku Y. VMA12 is essential for assembly of the vacuolar H(+)-ATPase subunits onto the vacuolar membrane in Saccharomyces cerevisiae. *J Biol Chem*. 1993;268:961–967.
9. Ichihara A, Hayashi M, Kaneshiro Y, Suzuki F, Nakagawa T, Tada Y, Koura Y, Nishiyama A, Okada H, Uddin MN, Nabi AH, Ishida Y, Inagami T, Saruta T. Inhibition of diabetic nephropathy by a decoy peptide corresponding to the "handle" region for nonproteolytic activation of prorenin. *J Clin Invest*. 2004;114:1128–1135.
10. Advani A, Kelly DJ, Cox AJ, White KE, Advani SL, Thai K, Connelly KA, Yuen D, Trogadis J, Herzenberg AM, Kuliszewski MA, Leong-Poi H, Gilbert RE. The (Pro)renin receptor: site-specific and functional linkage to the vacuolar H+-ATPase in the kidney. *Hypertension*. 2009;54:261–269.

Novelty and Significance

What is Known?

- (Pro)renin receptor [(P)RR], which plays a key role in the local renin-angiotensin system, is encoded by the *ATP6AP2* gene.
- The gene product of *ATP6AP2* is also associated with V-ATPase, which maintains an acidic environment in the lumen of intracellular vesicular compartments.

What New Information Does This Article Contribute?

- Cardiomyocyte-specific ablation of *Atp6ap2* caused fulminant heart failure.
- Ablation of *Atp6ap2* selectively suppressed protein expression of the V_0 subunits of V-ATPase, resulting in deacidification of intracellular vesicles.
- The phenotypes observed after genetic ablation of *Atp6ap2* are ascribed to V-ATPase loss of function.

The gene products of *ATP6AP2* have 2 distinct functions. Their first role in regulating the renin-angiotensin system pathway is well established, but a secondary role in regulating V-ATPase (and other cellular roles) has not been proposed or investigated in vivo. In the present study, we generated a mouse with a cardiac-specific deficiency in *Atp6ap2*. The *Atp6ap2*-disrupted cardiomyocytes showed extensive vacuolation, a phenotype that could be reproduced by pharmacologically inhibiting intracellular acidification. We demonstrated for the first time that ATP6AP2 might be an essential assembly chaperone of mammalian V-ATPase and that genetic ablation of *Atp6ap2* created a loss-of-function model for V-ATPase.

Supplement Material

Full Methods

Animals. All animal experiments were reviewed and approved by the Institutional Animal Care and Use Committee at the Keio University School of Medicine.

Generation of Atp6ap2 conditional knockout mice. The 13.3-kb genomic fragment that contains exons 2 and 3 of the *Atp6ap2* gene was obtained from a mouse BAC clone (RP23-339K2). A targeting vector was designed to insert a *loxP*- and *frt*-flanked PGK-*neo* cassette upstream of exon 2, and a third loxP site downstream of exon 2 of the targeted gene. The targeting vector was electroporated into C57/BL6 (B6) mouse-derived embryonic stem (ES) cells. Correctly targeted ES cells were injected into recipient blastocysts, and chimeric mice were bred with C57BL/6 mice, to establish a colony. The mutant mice were then bred with mice that expressed the Flp recombinase, to remove the *frt*-flanked *neo* cassettes. The resulting male *Atp6ap2*flox/Y mice (with loxP sites and a single Frt site remaining upstream of exon 2, and a second loxP site located downstream of exon 2) were bred with female mice that expressed cell-type-specific Cre recombinase.

Cardiomyocyte culture. Neonatal ventricular myocytes from 1- to 2-day-old Sprague-Dawley rats were subjected to Percoll gradient centrifugation and differential plating in order to enrich for cardiac myocytes and deplete nonmyocyte populations.[1]

Histology. Hearts were fixed overnight in 10% formalin at 4°C, dehydrated with 70% ethanol, mounted in paraffin, and sectioned (5-μm thickness). Heart sections were stained with hematoxylin and eosin (HE) or with Masson trichrome for fibrosis.[2] Low and high-magnification fields of short-axis views were analyzed using a BIOREVO (BZ-9000; Keyence, Japan).

For immunostaining, hearts were fixed in 4% paraformaldehyde, then successively infiltrated with 30% sucrose in PBS, embedded in OCT compound (Miles), and stored frozen. Sections of 6 micrometer thickness were mounted on gelatin-coated slides, and then stained with hematoxylin. Sections were stained immunochemically as described previously.[3] The immunnofluorescence of cultured cells were performed as previously described.[4] For the labeling of acidic organelles, cells were incubated with LysoTracker (Molecular Probes) for 30 minutes, and then fixed with 4% paraformaldehyde in PBS (pH 7.4). Fluorescence images were acquired with a confocal microscope, LSM 510 (Carl Zeiss).

For transmission electron microscopy, tissue was minced and fixed in 2% paraformaldehyde, 2.5% glutaraldehyde, and 0.1 M cacodylate buffer, prepared according to standard protocol; and

electron microscopy was performed using the RMC MT6000 ultramicrotome, and visualized using the Hitachi H7500 electron microscope and the 2K × 2K Gatan CCD camera.

For sequential time-lapse microscopic analysis, bafilomycin A1-, chloroquine-, or vehicle-treated cardiomyocytes were observed every 20-30minutes over 48-72 hours using Leica FW4000.

Antibodies. Antibodies against V-ATPase a subunits and RAB7 were described previously.[5-8] Other primary antibodies used were monoclonal antibodies for LAMP2 and actin (DSHB and Abcam, respectively), anti-tubulin and GAPDH antibody (Cell Signaling Technology), anti-ATP6AP2 antibody (R&D Systems), anti-p62 C terminus polyclonal antibody (Progen), anti-LC3 (kind gift from Dr. Komatsu, the Tokyo Metropolitan Institute of Medical Science). Fluorescent dye or enzyme-linked secondary antibodies were obtained from Jackson ImmunoResearch.

Gene expression. Total RNA was purified using TRIzol reagent according to manufacturer's instructions. For RT-PCR, total RNA was used for reverse transcriptase using random hexamer primers. Quantitative real-time PCR was performed using the ABI Prism 7700 sequence detection system (Applied Biosystems). Predesigned gene-specific primer and probe sets (TaqMan Gene Expression Assays) were used. The 18s ribosomal RNA was amplified as an internal control.

Western blotting. Protein lysate preparation and immunoblotting procedures were performed as previously described.[9] Total lysates were applied at 10-20 μg/lane on 5-20% gradient polyacrylamide gel (Daiich Pure Chemicals) and transferred to PVDF membrane with 0.2 μm pore size. The immunoblots were performed with aforementioned antibodies. Dulbecco's modified Eagle medium (DMEM), minimal essential medium (MEM) and fetal bovine serum (FBS) were from Invitrogen. The protein blot was developed with an ECL detection kit (GE Healthcare) or chemiluminescence (Amersham Biosciences), and images were obtained using an image capture system (model LAS1000 and LAS3000 luminoimager; Fujifilm). The intensities of bands were measured and analyzed using Image Gauge Software (Fujifilm).

Echocardiography. Mice were anesthetized by inhalation of 1.5% isoflurane, and then immobilized on a positionable platform in the supine position. Short-axis echocardiography and Doppler echocardiographic measurements were made using the Vevo 660 system (VisualSonics) with a 600 series real-time microvisualization scanhead probe.[2] The left ventricular (LV) internal end-systolic diameter and LV end-diastolic diameter (LVESD and LVEDD, respectively) were measured using the leading-edge convention adopted by the American Society of Echocardiography. LV fractional shortening (FS) was calculated according to the formula: FS (%) = [(LVEDD –

LVESD)/LVEDD] × 100.

Statistics. Values are presented as mean ± SEM. Statistical significance was evaluated using 2-tailed, unpaired Student's *t* tests for comparisons of 2 mean values. Multiple comparisons involving more than 3 groups were performed using ANOVA. A P value less than 0.05 was considered statistically significant.

Online Figure Legends

Online Figure I

Strategy used to generate a conditional *Atp6ap2* allele. The genomic structure, targeting vector, and targeted allele are shown. CDS, coding sequence; UTR, untranslated region; FRT, flipase recognition target.

Online Figure II

Female *Atp6ap2*-floxed mice were bred with male mice that expressed the Cre recombinase under the control of the cardiomyocyte-specific α-myosin heavy chain (αMHC) promoter.

Online Figure III

Ultrastructure of ATP6AP2-depleted cardiomyocytes. **a**, A giant autophagolysosome with undigested cytosolic constituents. **b**, A cytosolic inculusion composed of concentric lamellae body which is often found in lysosomal disease and chloroquine induced cardiomyopathy (arrow) **c**, Mitophagy (arrowhead). Scale bars: 1 μm.

Online Figure IV

a, PCR genotyping of MEF DNA reveals a deletion of floxed *Atp6ap2* contingent on coinheritance of Cre recombinase. **b**, Quantitative PCR analysis reveals ≥90% elimination of *Atp6ap2* from floxed MEFs after Ad-Cre treatment.

Online Figure V

Pharmacologic inhibition of intracellular acidification significantly up-regulates *Atp6ap2* mRNA expression in cultured cardiomyocytes. $*P < 0.05$ vs. WT control (unpaired Student's *t*-test).

Online Video Legends

Online Video I

Echocardiographic data in WT (**a**) and cardiomyocyte-specific *Atp6ap2* CKO (**b**) mice on PD18. Echocardiography measurements using left ventricular trace on B-mode images depicts severely impaired ventricular function.

Online Video II

Sequential time-lapse observation of the cultured cardiomyocytes. **a,** Cardiomyocytes treated with vehicle. **b**, Cardiomyocytes treated with bafilomycin A1. **c**, Cardiomyocytes treated with chloroquine. Time scale: 6 hours per second.

Supplementary References

1. Tokudome S, Sano M, Shinmura K, Matsuhashi T, Morizane S, Moriyama H, Tamaki K, Hayashida K, Nakanishi H, Yoshikawa N, Shimizu N, Endo J, Katayama T, Murata M, Yuasa S, Kaneda R, Tomita K, Eguchi N, Urade Y, Asano K, Utsunomiya Y, Suzuki T, Taguchi R, Tanaka H, Fukuda K. Glucocorticoid protects rodent hearts from ischemia/reperfusion injury by activating lipocalin-type prostaglandin D synthase-derived PGD2 biosynthesis. *J Clin Invest.* 2009;119:1477-1488.
2. Endo J, Sano M, Katayama T, Hishiki T, Shinmura K, Morizane S, Matsuhashi T, Katsumata Y, Zhang Y, Ito H, Nagahata Y, Marchitti S, Nishimaki K, Wolf AM, Nakanishi H, Hattori F, Vasiliou V, Adachi T, Ohsawa I, Taguchi R, Hirabayashi Y, Ohta S, Suematsu M, Ogawa S, Fukuda K. Metabolic remodeling induced by mitochondrial aldehyde stress stimulates tolerance to oxidative stress in the heart. *Circ Res.* 2009;105:1118-1127.
3. Endo J, Sano M, Fujita J, Hayashida K, Yuasa S, Aoyama N, Takehara Y, Kato O, Makino S, Ogawa S, Fukuda K. Bone marrow derived cells are involved in the pathogenesis of cardiac hypertrophy in response to pressure overload. *Circulation.* 2007;116:1176-1184.
4. Sun-Wada GH, Imai-Senga Y, Yamamoto A, Murata Y, Hirata T, Wada Y, Futai M. A proton pump ATPase with testis-specific E1-subunit isoform required for acrosome acidification. *J Biol Chem.* 2002;277:18098-18105.
5. Nakamura N, Yamamoto A, Wada Y, Futai M. Syntaxin 7 mediates endocytic trafficking to late endosomes. *J Biol Chem.* 2000;275:6523-6529.
6. Toyomura T, Oka T, Yamaguchi C, Wada Y, Futai M. Three subunit a isoforms of mouse vacuolar H(+)-ATPase. Preferential expression of the a3 isoform during osteoclast differentiation. *J Biol Chem.* 2000;275:8760-8765.
7. Nakamura N, Sun-Wada GH, Yamamoto A, Wada Y, Futai M. Association of mouse sorting nexin 1 with early endosomes. *J Biochem.* 2001;130:765-771.
8. Sun-Wada GH, Wada Y, Futai M. Lysosome and lysosome-related organelles responsible for specialized functions in higher organisms, with special emphasis on vacuolar-type proton ATPase. *Cell Struct Funct.* 2003;28:455-463.
9. Sano M, Tokudome S, Shimizu N, Yoshikawa N, Ogawa C, Shirakawa K, Endo J, Katayama T, Yuasa S, Ieda M, Makino S, Hattori F, Tanaka H, Fukuda K. Intramolecular control of protein stability, subnuclear compartmentalization, and coactivator function of peroxisome proliferator-activated receptor gamma coactivator 1alpha. *J Biol Chem.* 2007;282:25970-25980.

Online Figure I

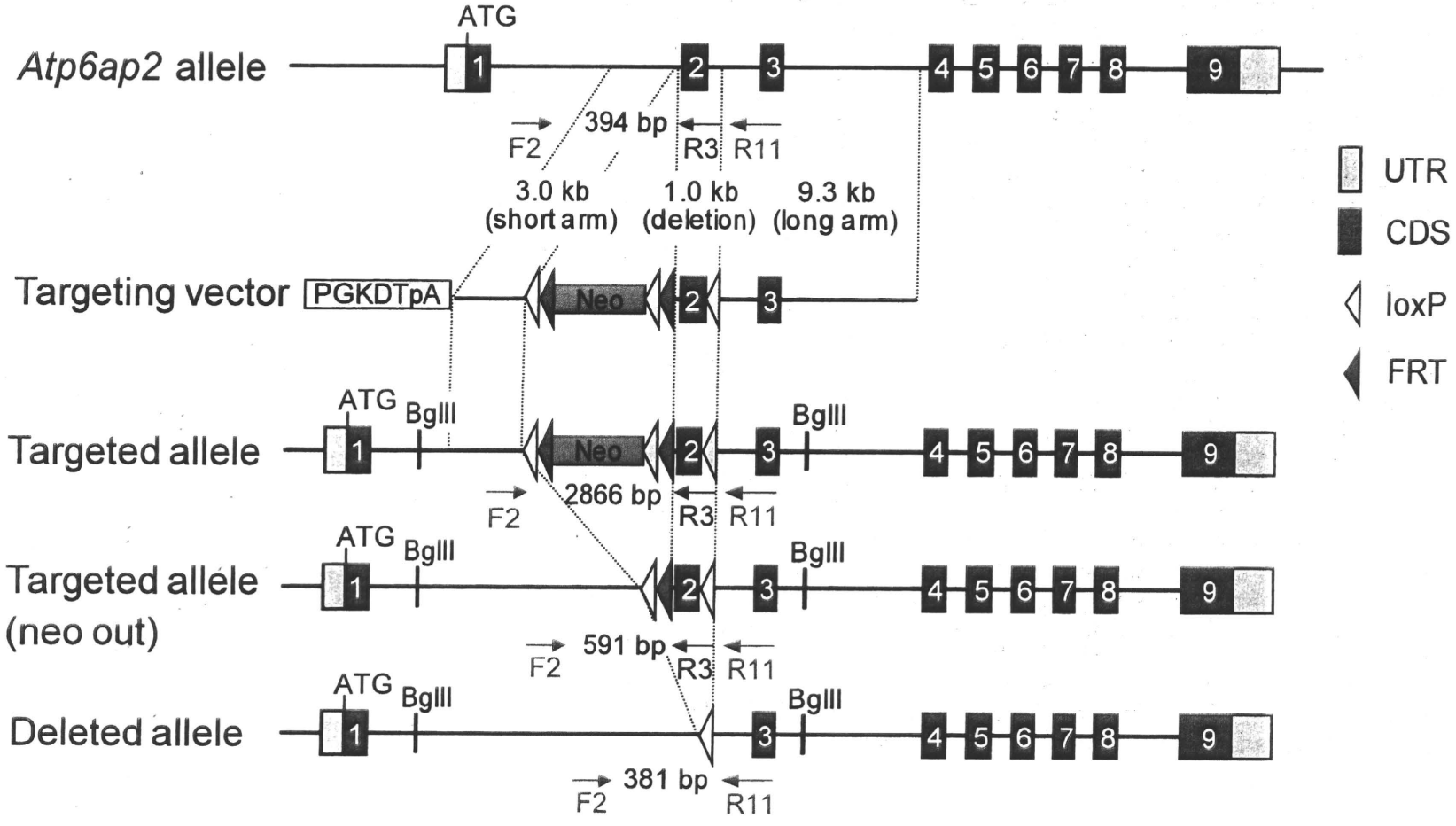

Online Figure II

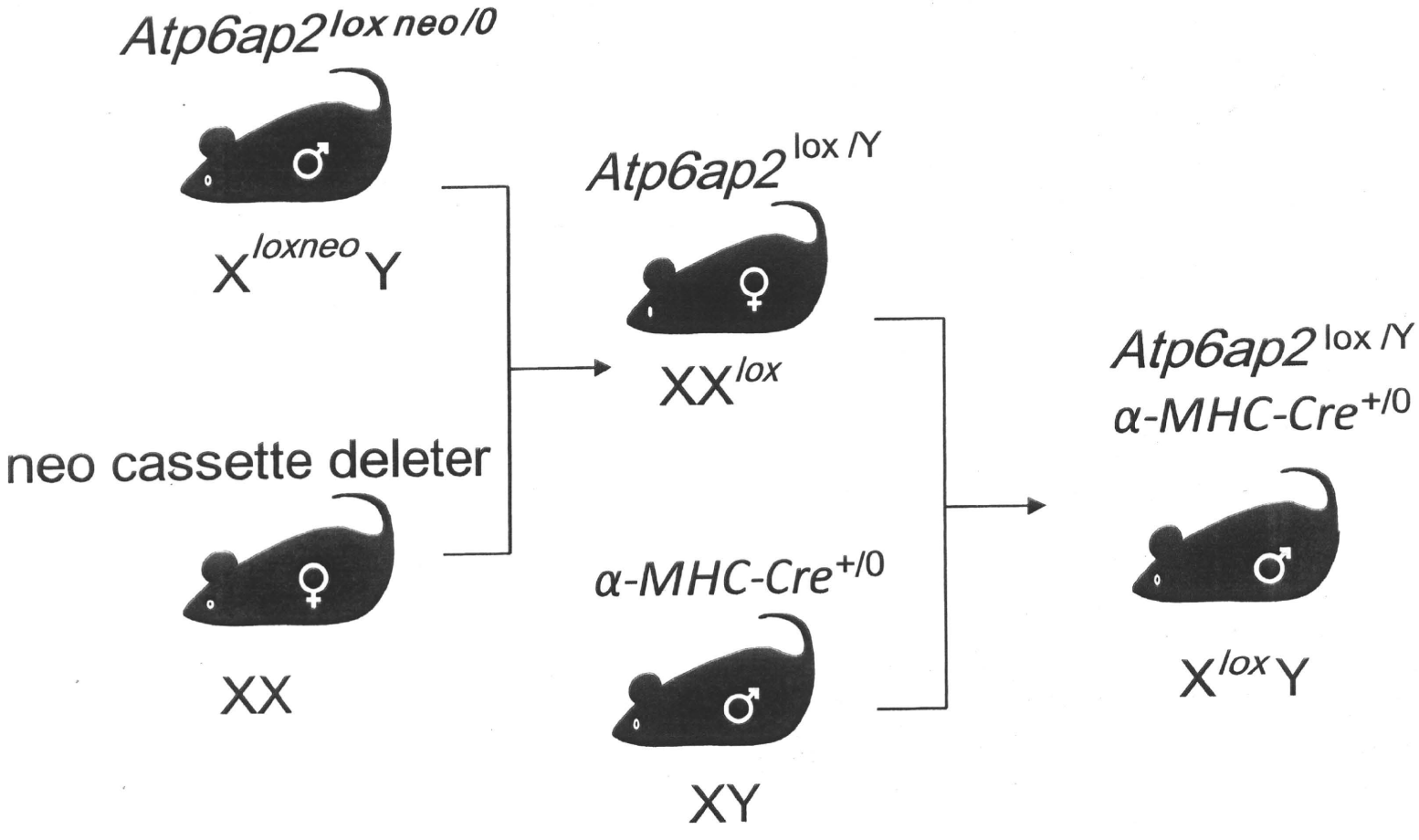

Online Figure III